The Influence of Axial Dispersion on Carbon Dioxide Absorption Tower Performance

MICHAEL I. BRITTAN and EDWARD T. WOODBURN

University of the Witwatersrand, Johannesburg, South Africa

Carbon dioxide was absorbed from mixtures with nitrogen by countercurrent contact with water in an experimental packed tower. Radial and axial gas concentration profiles were determined from measurements made within the packing. Substantial gas phase channeling was observed. Characterizing the gas flow regime by both piston flow and axial diffusion models yielded mass transfer data and computed axial gas concentration profiles. Differences between the mass transfer results for the two models allowed the influence of axial dispersion to be assessed. Comparison of the piston flow and axially dispersed profiles with the experimental profiles enabled conclusions to be drawn regarding the applicability of the axial diffusion model and the accuracy of available dispersion parameter values.

The axial diffusion model appears to be a satisfactory representation of the process. The dispersion coefficients used were found to be too high, which emphasizes shortcomings in the transient response experiments yielding dispersion coefficients. The influence of dispersion on the performance was found to be only moderately adverse. The effect increases with increasing liquid rate, decreasing gas rate, and decreasing packing height. It is improbable that the effect is large enough to account for the difference between industrial scale performance and that predicted from available mass transfer correlations.

The spread of fluid element residence times prevailing in an absorption tower invalidates the piston flow assumption inherent in existing design techniques. The resulting longitudinal dispersion will, in some measure, have an adverse influence on the performance. The magnitude of this effect has not as yet been determined, however. For carbon dioxide absorbers, in particular, it has been speculated that the wide discrepancy between the actual industrial scale performance and that predicted from standard mass transfer correlations (*19, 28, 31*) is due to axial dispersion of the gas phase. In two-phase operation of this nature, substantial gas phase mixing will be induced by the countercurrent liquid flow, particularly at the high water rates necessary to achieve satisfactory absorption of relatively insoluble gases such as carbon dioxide. Published gas-side dispersion coefficients for two-phase operation are scarce, but those available (*11, 12*) would indicate the effect of dispersion on the performance to be significant, especially if projected into the range of industrial liquid rates. The values of dispersion coefficients such as these, obtained from transient response experiments, have not been verified by application to steady state systems of practical interest. Consequently, their accuracy is subject to some question, and they cannot be employed to make definitive predictions.

The study described in this paper presents data to indicate the degree to which axial dispersion will affect absorption tower performance. By using published dispersion coefficients, the investigation serves also as a test of their accuracy. The evidence upon which the conclusions are based was obtained through measurement of axial gas concentration profiles in an experimental packed tower. Radial concentration profiles yielded at the same time throw some light on the flow of gases in irrigated packing. The data obtained serve also to elucidate the effects at the packing boundaries resulting from the dispersion.

Michael I. Brittan is at Yale University, New Haven, Connecticut. Edward T. Woodburn is at the University of Natal, Durban, South Africa.

DISPERSION CHARACTERIZATION

A number of models have been postulated to describe the mixing characteristics observed in continuous flow equipment (*18, 23*). The fundamental axial diffusion model has been employed in this study. The gross flow pattern is then represented by a superimposition of this diffusion mechanism on the uniform velocity of the fluid as it traverses the packed bed. This model represents an idealized situation, and it cannot be expected to account completely for the complex behavior of fluids in packed beds. The existence of nonflat velocity profiles in single-phase flow has been demonstrated (*5, 30*). For mixed phase gas-liquid operation, even greater deviation from a dispersed plug-flow concept is inevitable on the gas side. The presence of capacitive regions has also been inferred and verified (*7, 10, 16, 20, 21, 32*). Characterization of each of these effects would require a more comprehensive model (*23*) with a greater number of parameters. Consequently, the single parameter of the diffusion model will reflect the influences of all aberrations from the ideal postulates of the model.

It may be expected that the different regimes compounding the overall flow environment do not exhibit the same behavior under steady and unsteady state operating conditions. The importance of this lies in the fact that single axial dispersion parameters are determined from transient measurements, whereas their practical application is generally to steady state processes. Illustration is afforded by the computational fixed-bed reactor model of Deans and Lapidus (*10*). For their dynamic liquid phase studies, introduction of an additional parameter account-

ing for a capacitive effect was necessary to predict published Peclet numbers. Under steady state operation, an equilibrium concentration of solute would be maintained in the capacitance regions, thus rendering them unavailable for mass transfer. In the unsteady state, however, mass exchange by diffusion would occur with these regions, thus requiring an additional degree of freedom in the model to account for this. Gottschlich (*16*) similarly indicates that the stagnant film considered in his analysis will influence dispersion only in the unsteady state.

Conclusions as to the suitability of the axial diffusion model to describe the process will be drawn from the experimental results.

PROCESS FORMULATION

Complete characterization of the fluid dynamic behavior for the present system would require treatment of the dispersion occurring in both phases. Reviews of reported dispersion data (*10, 16, 17, 23*) reveal liquid flow axial Peclet numbers to be generally lower than the corresponding single-flow gas phase values. However, various workers have indicated that the liquid system results are evidently anomalous, with fluid capacitance being advanced as the probable cause (*7, 10, 13* to *16*). If this capacitive effect is dependent on diffusion of solute in the stagnant regions, then it can be expected that the difference between gas and liquid phase dispersion measurements will reflect the difference in the rates of diffusion in the two phases. The contribution of a diffusional mechanism to the measured variability of liquid residence-time distributions has been demonstrated (*14*). In the case of the model of Deans and Lapidus (*10*), the difference between gas and liquid phase data could in fact be reconciled by a contribution dependent on the diffusivity. Thus the comparatively sluggish diffusion in the liquid has a substantial influence on the transient response, whereas that of the rapid gas phase diffusion is minimal, as is suggested by the single-flow results of McHenry and Wilhelm (*25*) and of Sinclair and Potter (*33*). The apparent decrease of liquid phase dispersion noted with increasing liquid rate (*7, 12, 13, 22*) is also consistent with the disappearance of stagnant backwaters due to increased turbulence as the liquid rate is raised (*14*). Introduction of a stagnant film parameter into the model, as in the treatment of Gottschlich (*16*), reduced the actual degree of liquid dispersion to the magnitude of that for single-phase gaseous systems. Under these circumstances, axial dispersion would have a negligible effect on mass transfer.

Under conditions of irrigation, the degree of gas phase dispersion will increase because of additional friction between the gas and the opposing liquid flow. In these circumstances reported gas phase Peclet numbers (*11, 12*) are considerably lower than single-flow values in the absence of irrigation. It appears then that the relatively high degrees of gas phase mixing under irrigated conditions allow safe neglect of the influence of liquid phase dispersion.

A steady state material balance over an elemental tower length incorporating gas phase axial dispersion yields

$$\frac{d}{dZ}\left(-E\frac{dC_G}{dZ}\right)+\frac{d(uC_G)}{dZ}+K_L'a(C_L^*-C_L)=0 \quad (1)$$

where the primed notation on $K_L'a$ indicates a mass transfer coefficient isolated from the effects of dispersion.

In the experimental investigation no mass transfer was permitted to occur in the sections above and below the packing. The boundary conditions in this instance have been discussed by several workers referred to by Levenspiel and Bischoff (*23*) and are

$$Z=0: \qquad (uC_G)_{0-}=(uC_G)_{0+}-E\left(\frac{dC_G}{dZ}\right)_{0+} \quad (2)$$

$$Z=l: \qquad \frac{dC_G}{dZ}=0 \quad (3)$$

EFFECT OF THE TERMINAL CONDITIONS

The initial condition, Equation (2), represents a discontinuity in solute concentration at the inlet. Over a small section of packing at the entrance to the bed, this will result in a larger drop in concentration than would be the case in the absence of axial dispersion. Calculation of piston flow K_La values for a discrete packing entrance section will consequently provide higher values than those for comparable intermediate sections within the bed. At the outlet Equation (3) indicates an asymptotic approach to the exit concentration. In this region the concentration change over a discrete section of packing will be smaller than within the body of the packing. The corresponding K_La values will be lower if calculated on the assumption of piston flow. The two terminal manifestations of axial dispersion are thus seen to have opposing influences on axial concentration behavior.

EXPERIMENTAL

Carbon dioxide was absorbed from 20% mixtures with nitrogen by continuous countercurrent contact with water at 28°C. in a packed column. Henry's law solubility coefficient at this temperature was taken as the average of the value of Bohr (*3*) and that listed by Loomis (*24*). The resulting value of 1,767 atm./mole fraction agreed closely with that interpolated from the data of Morris and Jackson (*27*). The progress of the absorption was followed by sampling of gas at five intermediate axial locations within the packed bed, in addition to the two terminal sampling points. Thermal conductivity gas analysis was employed.

Liquid rates ranged between 5,517 and 9,195 lb./(hr.)(sq. ft.). Gas rates were selected in order to provide a satisfactory degree of absorption, advantageous from the viewpoint of accuracy, and representative of practical situations. The four gas feed rates employed were approximately 3.8, 5.8, 7.7, and 9.6 lb./(hr.)(sq. ft.). The operating variables thus correspond to ratios of L_M/G_M which range approximately from 1,300 to 5,160. Operating conditions of runs specifically referred to in Figures 2, 3, 5, and 6 are listed in Table 1.

Equipment

The absorption tower consisted of a single 3⅝ in. I.D. glass section. The overall packed height was 34.75 in. Sampling points were located at the following packing depths (in.): 3.15 (S1), 11.0 (S2), 16.9 (S3), 22.5 (S4), 30.75 (S5). The packing comprised ⅜ in. × ⅜ in. random glass Raschig rings. The normal wet-packing method was employed to pack the column. The tower-packing-diameter ratio was 9.7:1, satisfactorily above the generally accepted minimum of 8:1 proposed by Baker and co-workers (*1*) and close to the value of 10:1 suggested by Uchida and Fujita (*34*).

The gas inlet was inserted into the packing ½ in. above the grid support. A central inlet point was used after preliminary tests had shown that the position of the inlet along a diameter had no detectable effect on the performance. The liquid table level at the base of the packing was kept in contact with the packing support grid by means of a finely adjustable liquid

TABLE 1. OPERATING CONDITIONS OF RUNS SPECIFICALLY NOTED

Run No.	L, lb./(hr.)(sq. ft.)	Go, lb./(hr.)(sq. ft.)	P_T, mm. Hg
22	9195	9.58	623.5
30	7356	5.75	623.5
43	5517	5.76	624.1
73	6436.5	9.56	622.0

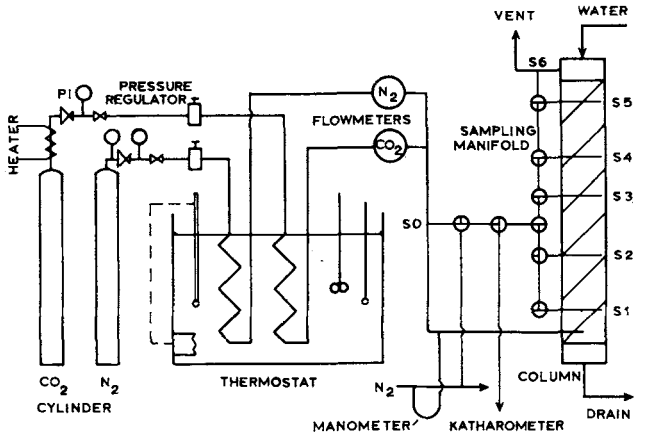

Fig. 1. Process gas supply circuit and gas sampling.

seal arrangement in the outlet line, thus minimizing any end effect. A level indicator insured the accurate and consistent placing of the water level. A substantial effort was made to eliminate physical end effects in the study. The presence of even a small unpacked space between the base of the packing and the liquid level was found to have a marked influence on the performance. Even though the insertion of the gas inlet into the packing eliminated a countercurrent spray zone below the packing, a considerable end effect would still be apparent (*4*).

Liquid entered the absorber from a small reservoir atop the column which fed the sixteen downcomers. A short liquid head above the downcomers sealed out air. The lower ends of the downcomers were placed in contact with the packing, thus eliminating any spray zone or splashing which could promote absorption, and obviating any possibility of surface tension effects at low liquid rates. A thermometer placed in the feed reservoir enabled the liquid temperature to be observed immediately prior to entry into the column.

Both gases were fed from cylinders. In the case of the carbon dioxide cylinder, a 75-w. heater was attached to the discharge line to prevent freezing of the gas due to the Joule-Thomson cooling effect of the expansion. The flow rates were controlled by precision pressure regulators. The gases flowed through coils immersed in a thermostat tank at the required experimental temperature. The flow rates were measured by manometric types of flowmeters. The gases combined after passage through the flowmeters and then entered the absorber. Figure 1 is a representation of the flow system. The process water supply circuit (not shown) was designed to provide a constant flow rate of water at a temperature which did not deviate by more than 0.1°C. from the desired value.

Gas rather than liquid phase analysis was employed, since it is simpler, continuous, and considerably more accurate than low concentration liquid determinations. Thermal conductivity measurements were made with a PYE twin-cell katharometer which was enclosed in a constant temperature environment and formed part of a Wheatstone network. A lamp-and-scale galvanometer registered the unbalance signals. The moisture content of the gas samples was taken into account in the analysis.

Gas sampling from within the packing raised the specific problem of obtaining a sample representative of the true mean gas composition at the cross section in question. Considerable deviation in the intermediate K_La values reported by Rixon (29) was attributed to the fact that sampling was effected at a single point within the packing rather than over an entire cross section. Preliminary tests in the present study showed that the composition along a diameter was far from uniform. The problem was to a large extent overcome by employing as the sampling probe two coaxial brass tubes, the outer of which remained fixed in the packing (to obviate disturbance of the packing configuration), while the inner was free to rotate. The outer tube was ⅜ in. O.D. to conform to the packing dimensions. Four 3/16 in. holes were drilled at points along its length. The inner tube (¼ in. O.D.) fitted snugly into the outer, the contact surface being greased to facilitate smooth rotation and to prevent the possibility of gas leakage. Four corresponding 3/16 in. holes were drilled on a spiral along the length of the inner tube, each displaced by 90 deg. from the adjacent hole. Thus 90-deg. rotation brought successive holes of the concentric tubes opposite one another, allowing any of the four radial positions to be selected.

The inner tubes were connected to the sampling manifold shown in Figure 1 by means of ground-glass capillary joints which permitted the required rotation. Capillary tubing was used throughout for the sampling lines. At the sampling rate of 20 cc./min. the maximum lag of gas elements before reaching the thermal conductivity cell was thereby kept down to a few seconds only. Samples were withdrawn by vacuum. Only in extremely rare instances was water sucked into the sampling tubes, thus preventing the reading being taken. The sampling rate was negligible in comparison with the overall gas flow rates employed. The arrangement of the sampling manifold is apparent in Figure 1 and rapid selection of any sampling point desired was possible.

Procedure

Refer to Figure 1. Water at the required flow rate and temperature was introduced to the tower. Liquid was allowed to pass through the absorber at the requisite rate for a considerable time period before taking readings. This insured that all parts of the column would be at the correct temperature and that liquid distribution and holdup on the packing were allowed sufficient time to reach steady state. The gas flows were set at the desired rates by means of the precision pressure regulators. The system was then left to attain steady state conditions with constant checks on the flow rates and temperature being made. During this period the thermal conductivity gas analysis circuit was brought into operation. Samples of column feed gas were analyzed and the zero setting was checked after each reading until consistency was obtained. Samples from each of the four radial positions at each packed height were drawn in turn by rotation of the concentric tube sampling probe. After each set of such readings, reference nitrogen was sampled to check the zero point. This was repeated until deviations between successive readings were eliminated. Barometric pressure was recorded during every run. Each run was normally repeated three times to assure reproducibility. Further equipment and procedural details are given by Brittan (*4*).

READINGS

Transverse and Axial Gas Concentration Profiles

The experimental readings consisted of the terminal gas compositions plus a series of transverse concentration profiles for five distributed axial positions. Typical transverse profiles are shown in Figures 2 and 3. The profiles are superimposed on coordinates representing longitudinal bed position as ordinate and diametral location on an exaggerated abscissa scale. This arrangement allows the profiles to be observed at varying bed depths. It is evident from Figures 2 and 3, as from all the results, that in general the radial concentrations become increasingly disperse as the packing depth traversed by the gas becomes greater. The profiles at the plane of S1 are reasonably flat, but at S5 the individual radial compositions can differ substantially from each other. A substantial degree of gas channeling in the course of passage up the tower is indicated, probably due to occlusion of the gas flow paths by the nonuniform liquid irrigation. From the results it also appeared that the dispersion increases as the liquid rate rises, a trend not unexpected from intuitive considerations.

To obtain the axial profiles, the four radial compositions at each sampling cross section were resolved into a single concentration representing the mean composition of the cross section.

CALCULATION OF MASS TRANSFER DATA

Piston Flow Model

With a piston flow model for the flow regime, the mass transfer quantities K_La and H_{OL} were evaluated from

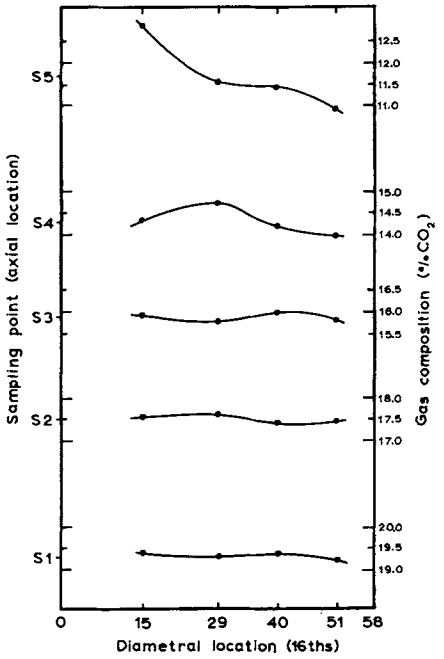

Fig. 2. Transverse concentration profiles. Run 43.

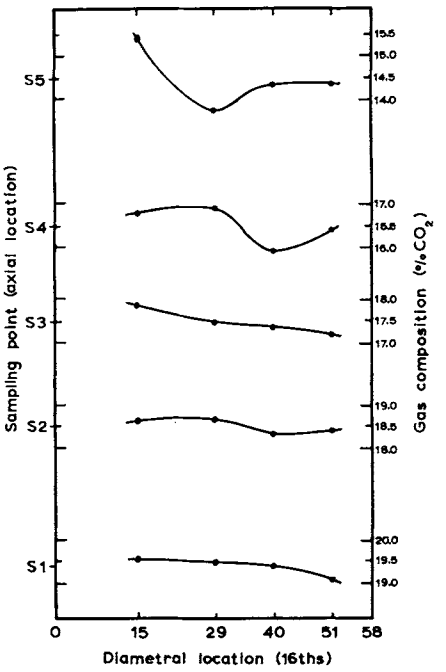

Fig. 3. Transverse concentration profiles. Run 73.

$$\int_{x_0}^{x_1} \frac{dX}{(X^* - X)} = \frac{K_L a \rho l}{L} = \frac{l}{H_{OL}} \qquad (4)$$

Material balances provided values of X from the experimental readings.†

For systems obeying Henry's law, such as that under investigation, an analytical solution to the integral of Equation (4) has been developed (*4*). The solution permits precise calculation of mass transfer quantities. Its use indicated that approximations such as equilibrium line linearity can lead to significant error where the degree of absorption is appreciable. The apparent mass transfer data yielded by this method were calculated for all the intermediate sections of packing and suitable composite combinations of these. For the present study the values for the overall (S0 to S6) and largest internal (S1 to S5) packed height are of interest. These are listed in Table 2 ($P \rightarrow \infty$ denotes piston flow). The variation with gas rate was small enough so that values averaged over all gas rates at each liquid rate were tabulated.

Axial Diffusion Model

In this case, solution of Equation (1) is required. With the liquid concentration terms of the equation transformed to functions of gas phase composition and the equation rendered dimensionless, the following differential equation is obtained (*4*):

$$\frac{d^2f}{dz^2} + \frac{y_0}{(1 - y_0 f)}\left(\frac{df}{dz}\right)^2 - \left\{\frac{P}{1 - y_0 f} + N'_{OL}\right\}\frac{df}{dz} - PN'_{OL}(1 - y_0 f)\left\{\frac{L_M P_T}{G_M' H} f - \frac{f}{1 - y_0 f} + \frac{f_1}{1 - y_0 f_1} - \frac{v_{CO_2} X_1 L_M}{v_{N_2} y_0 G_M'}\right\} = 0 \qquad (5)$$

The associated boundary conditions reduce to

$$z = 0: \quad f_{0+} = 1 + \frac{(1 - y_0)}{P}\left(\frac{df}{dz}\right)_{0+} \qquad (6)$$

$$z = 1: \quad (df/dz) = 0 \qquad (7)$$

The method of numerical solution of Equation (5) (which accounts for the decrease in gas flow rate due to adsorption) is described elsewhere (*4*).‡

The treatment was applied to those experimental conditions for which the mass transfer coefficient was relatively invariant over the internal packing sections. Available axial dispersion coefficients for the gas phase of continuous countercurrent operation were limited to those of DeMaria and White (*11*) and of Dunn et al. (*12*).

† For this purpose a knowledge of the free carbon dioxide content of the feed water was required. The difficulties of accurate analysis for minute quantities favored calculation from data supplied by the Rand Water Board. The value of X_1 thus obtained was 4.1×10^{-7} mole ratio carbon dioxide.

‡ The calculations referred to in the present study were based on an equation slightly different from (5). This resulted from the use of a constant value of E over the tower length. The effect on the computed data is inconsequential.

Table 2. Actual and Apparent Mass Transfer Data Averaged over All Gas Rates

L, lb./(hr.)(sq. ft.)		9,195		8,275.5		7,356		5,517	
		H_{OL}, ft.	$K_L a$, hr.$^{-1}$	H_{OL}, ft.	$K_L a$, hr.$^{-1}$	H_{OL}, ft.	$K_L a$, hr.$^{-1}$	H_{OL}, ft.	$K_L a$, hr.$^{-1}$
(S0 to S6)	P finite	2.48	59.7	2.46	54.2	2.24	52.8	1.88	47.4
(S0 to S6)	$P \rightarrow \infty$	2.75	53.9	2.64	50.5	2.39	49.6	1.95	45.5
	% diff.		10.6		7.3		6.5		4.1
(S1 to S5)	$P \rightarrow \infty$	2.64	56.0	2.48	53.7	2.45	48.3	1.97	45.0

TABLE 3. ACTUAL AND APPARENT MEAN MASS TRANSFER DATA

L, lb./(hr.)(sq. ft.)	Avg., G_O, lb./(hr.)(sq. ft.)	9.58		7.66		5.75		3.83	
		H_{OL}, ft.	K_La, hr.$^{-1}$	H_{OL}, ft.	K_La, hr.$^{-1}$	H_{OL}, ft.	K_La, hr.$^{-1}$	H_{OL}, ft.	K_La, hr.$^{-1}$
	$P = 9.5$	2.43	61.1	2.58	57.1	2.51	58.8	2.43	61.0
9,195	$P \rightarrow \infty$	2.59	57.2	2.78	53.2	2.79	53.1	2.85	51.9
	% diff.		6.8		7.3		10.9		17.5
	$P = 11.9$			2.55	52.3	2.37	56.0		
8,275.5	$P \rightarrow \infty$			2.70	49.4	2.58	51.6		
	% diff.				5.9		8.5		
	$P = 14.5$	2.11	56.1	2.29	51.6	2.28	51.9	2.29	51.7
7,356	$P \rightarrow \infty$	2.21	53.6	2.40	49.2	2.42	48.8	2.53	46.8
	% diff.		4.7		4.9		6.4		10.3
	$P = 21.3$	1.82	48.8	1.83	48.6	1.89	47.1	1.97	45.0
5,517	$P \rightarrow \infty$	1.87	47.5	1.89	47.1	1.97	45.1	2.09	42.4
	% diff.		2.7		3.2		4.4		6.3

The data of DeMaria and White were employed since they were determined with ⅜ in. ring packing and column dimensions similar to those of the present study. Conversion to the required axial dispersion groups was effected as follows:

$$E' = \frac{v'd_p}{N_{Pe}} = \frac{u'd_p}{\epsilon N_{Pe}}$$

$$P = \frac{u'l}{E'} = \frac{\epsilon N_{Pe} l}{d_p} = 92.6\,\epsilon N_{Pe}$$

A 40% linear extrapolation of the data presented by DeMaria and White was necessary to cover the range of liquid rates considered here. Values of P thus calculated are given in Table 3.

Evaluation of the number of transfer units N'_{OL}, satisfying simultaneously the model equation with a specified degree of axial dispersion, and the experimental results involved a trial-and-error procedure. Adjustment of N'_{OL} was required until the computed exit gas composition agreed with the experimental value. In addition to the reduced concentration profiles obtained, profiles for the corresponding hypothetical piston flow situations were also generated for comparison by the same procedure with large values of P.

COMPUTED RESULTS AND OBSERVATIONS

The data yielded for each of the experimental runs treated thus comprise: the true number of transfer units, denoted N'_{OL}; apparent N_{OL} values calculated on the assumption of piston flow; computed axial gas concentration profiles accounting for axial dispersion; and profiles computed on the basis of a piston flow model.

Mass Transfer Data

With H_{OL} and K_La data evaluated for the two cases of flow pattern represented by the axial diffusion and piston flow models, the mean values of the triplicate data for each set of experimental conditions are presented in Table 3. As is to be expected, the data of Table 3 indicate an adverse effect of gas phase axial dispersion on the absorber performance. The higher degrees of backmixing as the liquid rate is raised are reflected in the corresponding increase in differences between the mass transfer data based on piston flow and axially dispersed gas phase environs. It will be noted also that the differences increase with decreasing gas rate, that is, increasing degree of absorption. It serves to confirm the intuitive reasoning of Cooper, Christl, and Peery (9), that backmixing would be more detrimental to performance the greater the change in gas concentration over the absorption tower length. One consequence of this is that axial dispersion will contribute to any observed effect of gas rate on the performance.

To facilitate comparison, mass transfer data averaged over all the gas rates at each liquid rate were evaluated. These are listed in Table 2. The usual power function correlations were found adequate to represent the K_La data of Table 2 and were determined by the method of least squares. For the piston flow case, the apparent mass transfer coefficient is given by

$$K_La = 3.12\,(L)^{0.31} \tag{8}$$

With the effects of axial dispersion segregated from the process of mass transfer, the actual coefficient is represented by

$$K_L'a = 1.216\,(L)^{0.424} \tag{9}$$

The equation correlating the apparent mass transfer data for the intermediate packed section S1 to S5 is also presented. In effect, this provides a mass transfer coefficient calculated from a piston flow model but essentially free from the influence of the packing boundaries. In this case the relationship is

$$K_La = 1.107\,(L)^{0.43} \tag{10}$$

Equations (8), (9), and (10) refer to coefficients which are respectively analogous to the *exterior apparent, true,* and *interior apparent* values as designated by Miyauchi and Vermeulen (26) (through the interior apparent region discussed by these workers denotes the entire packed

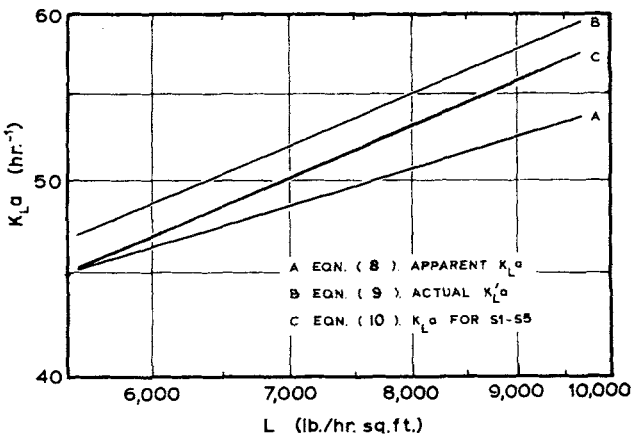

Fig. 4. Equations (8), (9), (10).

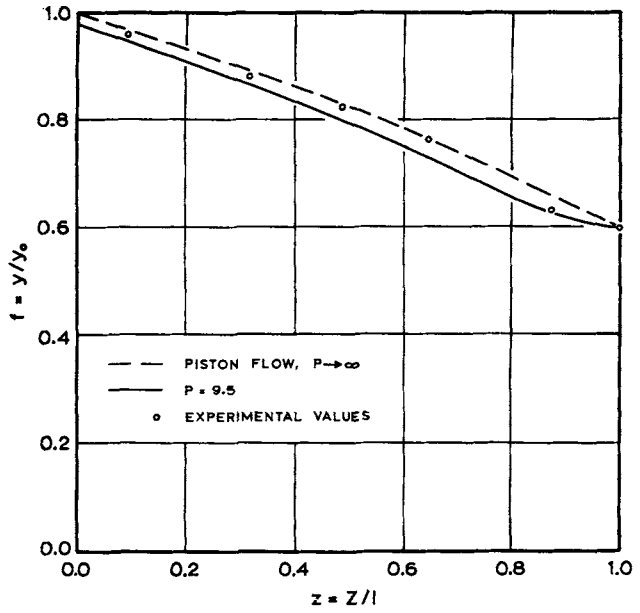

Fig. 5. Influence of axial dispersion on axial concentration profiles. Run 22.

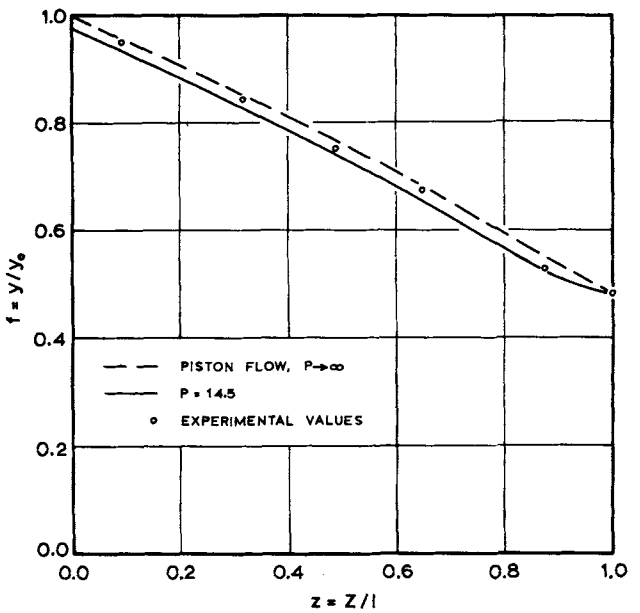

Fig. 6. Influence of axial dispersion on axial concentration profiles. Run 30.

height). The equations are compared graphically in Figure 4. The difference between the apparent and true mass transfer coefficients is not particularly large; however, the rate of its increase with liquid rate is appreciable. If the rate as indicated by Figure 4 were maintained, substantial deviation would result at higher liquid rates.

The similarity between Equations (9) and (10) will be noted. The difference between the two equations depends in part on the magnitude of the axial dispersion coefficients used to arrive at (9). The similarity is probably coincidental but nevertheless would suggest that the influence of axial dispersion on the performance is in some way related to the effects at the packing boundaries associated with the dispersion. In this regard Miyauchi and Vermeulen (*26*) have treated the inlet discontinuity in concentration as a measure of the influence of dispersion. It is apparent from Figure 4 that the performance evaluated from a piston flow calculation would display a lesser influence of axial dispersion if internally measured concentrations were used rather than concentrations external to the packing. However, the differences involved are too small and the present data insufficiently accurate to permit the establishment of quantitative conclusions in this regard.

The effects at the boundaries may conveniently be compared in magnitude by referring to the piston flow K_La data for the sections S0 to S1 and S5 to S6. These are listed by Brittan (*4*) and comprise one hundred thirty-eight readings additional to those considered in this paper. The data are somewhat scattered due to the difficulties associated with gas sampling from within the packing. Nevertheless the tendency toward higher K_La values at the gas inlet and lower at the outlet is clearly apparent. This is in accordance with the predictions of the axial diffusion model and verifies that dispersion does in fact occur. The gross influence on the performance of the opposing terminal phenomena is reflected in the difference between the performance for the overall (S0 to S6) and intermediate (S1 to S5) packing sections. Some of the data are represented in smoothed fashion by the difference between lines *A* and *C* of Figure 4. Indications are that the difference rises as the liquid rate increases, suggesting that the exit terminal effect predominates at higher liquid flow rates.

Axial Gas Concentration Profiles

Presented in Figures 5 and 6 are typical reduced concentration profiles abstracted from the computed data. The profiles are shown for the two conditions of gas phase flow described by the piston flow and axial diffusion models. Superimposed are the experimental points. In general, the experimental values are seen to fall between the two profiles. (It should be pointed out that a single average mass transfer coefficient was used to generate each computed profile even though small variations in the coefficient along the tower length were encountered.) The measured points are, if anything, somewhat closer to the piston flow situation. This serves to indicate that the axial dispersion coefficients of DeMaria and White (*11*) actually are too high to represent satisfactorily the countercurrent mass exchange system considered here. As they stand, the dispersed flow profiles do provide an indication as to the axial concentration behavior which can be expected for greater degrees of gas phase stirring than experienced in this investigation. Such would be the case for operation at higher liquid flow rates.

DISCUSSION AND CONCLUSIONS

The results obtained may be used to assess the suitability of the axial diffusion model as a representation of the longitudinal dispersion phenomena occurring in the steady state absorption process investigated. Though a single-parameter model of this nature is an idealization, it should be adequate for all practical steady state purposes, provided that satisfactory values of E are available. The model and its boundary conditions appear consistent with the experimentally observed lowering of the axial concentration profile from that which would prevail if piston flow were possible.

The inability of the dispersion data employed to describe satisfactorily the measured results emphasizes the need for critical evaluation of the transient analyses which yield the parameters. The sensitivity of the calculated parameters to the method of determination and associated experimental details has been noted (*6*). Of special importance is an appreciation of the fact that the influence of such factors as fluid capacitance may not be common to dynamic and steady state operation. Since the ultimate

application of dispersion data is usually to steady state systems, distinctions between steady and unsteady state situations must be accounted for. Single-parameter diffusion mechanisms are not generally adequate to characterize transient measurements, as has recently been observed (*20*). On the other hand, such mechanisms appear to be satisfactorily commensurate with steady state behavior. Another factor of significance is the effect on transient breakthrough measurements of inevitable fluid channeling. Cairns and Prausnitz (*6*) have shown that where nonflat velocity profiles exist, radially integrated breakthrough curves can result in misleadingly low Peclet numbers. Point measurements are necessary to avoid this, a factor which has not generally been appreciated in the determination of axial dispersion coefficients from transient response experiments. The effect of velocity profiles on axial mixing in packed beds has also been demonstrated by Converse (9). In this context the effect on transient determinations of the substantial gas phase channeling witnessed in the present study can be expected to be pronounced. In addition, an apparent variation of dispersion coefficient with bed length could result. End effects will also have measurable influence on transient response measurements. These must be eliminated as far as possible or satisfactorily accounted for (*2*).

The axial dispersion coefficients employed were proven to be too high in value. In other words, an overspecified degree of dispersion was used in the calculations. Consequently, the actual coefficients of mass transfer $K_L'a$, obtained from the experimental readings, are somewhat too large. With this in mind, axial dispersion has only a moderately small detrimental influence on the performance of the absorption tower used in the range of operating conditions studied.

As has been noted in previous publications concerning continuous flow equipment, the effect of dispersion increases with increasing degree of absorption (that is, decreasing gas rate) and may be significant in processes where substantial removal of solute from the gas phase is required. Much previous mass transfer work has entailed stripping operation at high gas rates. The resulting gas compositions should in most cases be small enough to minimize the influence of axial dispersion on the performance. The effect also increases with increasing liquid rate and decreasing packing height (the axial dispersion group $P = u'l/E'$ being directly dependent on l). Variations in liquid rate and packing height will, moreover, be attended by changes in the degree of absorption.

It was mentioned earlier that axial dispersion has been considered responsible for the marked difference between the performance of industrial carbon dioxide absorbers and that predicted from experimental scale results. In view of the conclusions reached in the investigation, and noting the differences in conditions between small and industrial scale operation, axial dispersion would appear to constitute only a relatively small part of the cause of the discrepancy.

ACKNOWLEDGMENT

The authors acknowledge the helpful discussions with Dr. R. P. King of the University of the Witwatersrand, and the advice of Dr. M. M. Wendel of E. I. duPont de Nemours and Company, Gibbstown, New Jersey, concerning the numerical solution. The financial assistance of the South African Council for Scientific and Industrial Research and the facilities of the University Computing Centre are gratefully appreciated.

NOTATION

C_G = gas phase solute concentration, mole/cu. ft.
C_L = liquid phase solute concentration, mole/cu. ft.
C_L^* = equilibrium liquid phase solute concentration, mole/cu. ft.
d_p = characteristic packing dimension, ft.
E = axial dispersion coefficient at total gas velocity, sq. ft./hr.
E' = axial dispersion coefficient at inert gas velocity, sq. ft./hr.
f = reduced gas phase concentration, y/y_0
G = superficial mass gas rate, lb./(hr.)(sq. ft.)
G_M = superficial molar gas rate, lb.-mole/(hr.)(sq. ft.)
G_M' = superficial inert molar gas rate, lb.-mole/(hr.)(sq. ft.)
H = Henry's law solubility coefficient, atm./mole fraction or mm./mole fraction
H_{OL} = apparent height of an overall transfer unit, ft.
K_La = apparent capacity overall transfer coefficient, lb.-mole/(hr.)(cu. ft.)(lb.-mole/cu. ft.)
$K_L'a$ = actual capacity overall transfer coefficient, lb.-mole/(hr.)(cu. ft.)(lb.-mole/cu. ft.)
l = total height of packing, ft.
L = superficial mass liquid rate, lb./(hr.)(sq. ft.)
L_M = superficial molar liquid rate, lb.-mole/(hr.)(sq. ft.)
N_{OL} = apparent number of overall transfer units
N'_{OL} = actual number of overall transfer units
N_{Pe} = Peclet number, (vd_p/E)
P = axial dispersion group, $(u'l/E')$
P_T = total pressure, atm. or mm. Hg
u = superficial gas velocity, $v\epsilon$, cu. ft./(hr.)(sq. ft.)
u' = superficial inert gas velocity, cu. ft./(hr.)(sq. ft.)
v = gas velocity, ft./hr.
v' = inert gas velocity, ft./hr.
v_{N_2}, v_{CO_2} = specific volume, cu. ft./lb.-mole
X = solute concentration in liquid phase, lb.-mole solute/lb.-mole solvent
X^* = equilibrium solute concentration in liquid phase, lb.-mole solute/lb.-mole solvent
y = volume fraction solute in gas phase
z = reduced axial coordinte, Z/l
Z = axial coordinate, ft.

Greek Letters

ϵ = void fraction, cu. ft./cu. ft.
ρ = density, lb./cu. ft.

Subscripts

0 = lower terminal condition
1 = upper terminal condition

LITERATURE CITED

1. Baker, T., T. H. Chilton, and H. C. Vernon, *Trans. Am. Inst. Chem. Engrs.*, **31**, 296 (1935).
2. Bischoff, K. B., and O. Levenspiel, *Chem. Eng. Sci.*, **17**, 245 (1962).
3. Bohr, C., *Anal. Phys.*, **68**, 500 (1899); see "International Critical Tables," Vol. 3, p. 260, McGraw-Hill, New York (1928).
4. Brittan, M. I., M.Sc. thesis, Univ. Witwatersrand, Johannesburg, South Africa (1964).
5. Cairns, E. J., and J. M. Prausnitz, *Ind. Eng. Chem.*, **51**, 1441 (1959).
6. ————, *Chem. Eng. Sci.*, **12**, 20 (1960).
7. Carberry, J. J., and R. H. Bretton, *A.I.Ch.E. J.*, **4**, 367 (1958).
8. Converse, A. O., *ibid.*, **6**, 344 (1960).
9. Cooper, C. M., R. J. Christl, and L. C. Peery, *Trans. Am. Inst. Chem. Engrs.*, **37**, 979 (1941).
10. Deans, H. A., and Leon Lapidus, *A.I.Ch.E. J.*, **6**, 656, 663 (1960).
11. DeMaria, F., and R. R. White, *ibid.*, 473.
12. Dunn, W. E., Theodore Vermeulen, C. R. Wilke, and T. T. Word, *Univ. Calif. Rad. Lab. Rept. No. UCRL 10394* (1962).

13. Ebach, E. A., and R. R. White, *Chem. Eng. Progr.*, **4**, 161 (1958).
14. Glaser, M. B., and I. Lichtenstein, *A.I.Ch.E. J.*, **9**, 30 (1963).
15. Glaser, M. B., and Mitchell Litt, *ibid.*, 103.
16. Gottschlich, C. H., *ibid.*, 88.
17. Green, D. W., R. H. Perry, and R. E. Babcock, *ibid.*, **10**. 645 (1964).
18. Hoffman, H., *Chem. Eng. Sci.*, **14**, 193 (1961).
19. Hoftyzer, P. J., "Joint Symposium on Scaling-up," p. S73, Inst. Chem. Engrs., London (1957).
20. Hoogendoorn, C. J., and J. Lips, *Can. J. Chem. Eng.*, **43**, 125 (1965).
21. King, R. P., M.Sc. thesis, Univ. Witwatersrand, Johannesburg, South Africa (1962).
22. Kramers, H. and G. Alberda, *Chem. Eng. Sci.*, **2**, 173 (1953).
23. Levenspiel, O., and K. B. Bischoff, "Advances in Chemical Engineering," Vol. 4, p. 95, Academic Press, New York (1963).
24. Loomis, A. L., "International Critical Tables," Vol. 3, p. 260, McGraw-Hill, New York (1928).
25. McHenry, K. W., and R. H. Wilhelm, *A.I.Ch.E. J.*, **3**, 83 (1957).
26. Miyauchi, Terukatsu, and Theodore Vermeulen, *Ind. Eng. Chem. Fundamentals*, **2**, 113 (1963).
27. Morris, G. A., and J. Jackson, "Absorption Towers," p. 143, Butterworths, London (1953).
28. Norman, W. S., "Absorption, Distillation and Cooling Towers," pp. 192, 193, Longmans, London (1961).
29. Rixon, F. F., *Trans. Inst. Chem. Engrs. (London)*, **26**, 119 (1948).
30. Schwartz, C. E., and J. M. Smith, *Ind. Eng. Chem.*, **45**, 1209 (1953).
31. Sherwood, T. K., and R. L. Pigford, "Absorption and Extraction," 2 ed., p. 291, McGraw-Hill, New York (1952).
32. Shulman, H. L., C. F. Ullrich, A. Z. Proulx, and J. O. Zimmerman, *A.I.Ch.E. J.*, **1**, 253 (1955).
33. Sinclair, R. J., and O. E. Potter, *Trans. Inst. Chem. Engrs. (London)*, **43**, T3 (1965).
34. Uchida, S., and S. Fujita, *J. Soc. Chem. Ind. (Japan)*, Suppl., **37**, 274 (1934); **39**, 432 (1936); **41**, 275 (1938).

Manuscript received June 8, 1965; revision received January 5, 1966; paper accepted January 12, 1966. Paper presented at A.I.Ch.E. Philadelphia meeting.

Diffusion of Gases in Electrolytic Solutions

KEITH E. GUBBINS, KAMLESH K. BHATIA, and ROBERT D. WALKER, JR.

University of Florida, Gainesville, Florida

Measurements of the diffusion coefficients of hydrogen and methane in strong aqueous electrolytes have been made with the use of the diaphragm cell method. The variation of the diffusion coefficients with electrolyte concentration, type of ion, and temperature has been studied over the electrolyte concentration range zero to saturated, and for temperatures in the range 25° to 65°C.

The results have been interpreted with the Eyring rate theory. The presence of ions in water increases the activation energy for diffusion which results in a decrease in the diffusion coefficient. The increase in activation energy is represented by terms that are additive for the ions involved. The influence of ions on the diffusion coefficient increases rapidly with ionic charge, but seems to be little affected by temperature or solute for the systems studied.

The prediction of the rate of diffusion of nonelectrolytes through aqueous electrolytes is of interest in a number of practical problems, for example, the study of mass transfer limitations at electrodes. Although the Wilke-Chang equation (*1, 2*) provides a means of estimating binary diffusion coefficients in liquids, it is not immediately applicable to electrolytes, since it involves the solvent molecular weight and an association parameter. The Eyring theory (*3, 4*) of reaction rates provides a starting point for the development of correlations for diffusion in electrolytes, and has been used by Podolsky (*5*) and Ratcliff (*6*) in developing relationships for the fluidity of electrolytes and also for the diffusion of nonelectrolytes. Very few experimental studies of diffusion of dissolved gases in electrolyte solutions are available, and the measurements reported have been made at a single temperature (*6, 7*). The object of the present work is to examine the variation of gaseous diffusion coefficients with solute gas, electrolyte, concentration, and temperature.

K. K. Bhatia is with Procter and Gamble Company, Cincinnati, Ohio.

THEORY

According to the Eyring reaction rate theory, the fluidity of a liquid ϕ and the binary diffusion coefficient in dilute solution D are given by

$$\phi = \frac{1}{\eta} = k_\phi \lambda^2 e^{-\Delta G_\phi^*/RT} = k_\phi \lambda^2 \frac{h}{(2\pi mkT)^{1/2} v_f^{1/3}} e^{-\epsilon_\phi/kT} \quad (1)$$

$$D = k_d \lambda^2 e^{-\Delta G_d^*/RT} = k_d \lambda^2 \frac{h}{(2\pi mkT)^{1/2} v_f^{1/3}} e^{-\epsilon_d/kT} \quad (2)$$

Weyman (*8*) recently has derived equations similar to (1) and (2) by more rigorous statistical mechanical methods. The diffusion coefficient (or fluidity) is determined primarily by the activation energy for the process and the temperature.

Podolsky (*5*) has derived an expression for the fluidity of an electrolyte solution using Equation (1), and Ratcliff (*6*) has proposed a corresponding equation for the diffusion coefficients of gases in electrolytes. Their derivation is outlined below.